

Majorana dark matter through the Higgs portal under the vacuum stability lamppost

Luis A. Anchordoqui,^{1,2,3} Vernon Barger,⁴ Haim Goldberg,⁵ Xing Huang,⁶
Danny Marfatia,⁷ Luiz H. M. da Silva,⁸ and Thomas J. Weiler⁹

¹*Department of Physics and Astronomy, Lehman College, City University of New York, NY 10468, USA*

²*Department of Physics, Graduate Center, City University of New York, 365 Fifth Avenue, NY 10016, USA*

³*Department of Astrophysics, American Museum of Natural History, Central Park West 79 St., NY 10024, USA*

⁴*Department of Physics, University of Wisconsin, Madison, WI 53706, USA*

⁵*Department of Physics, Northeastern University, Boston, MA 02115, USA*

⁶*Department of Physics, National Taiwan Normal University, Taipei, 116, Taiwan*

⁷*Department of Physics and Astronomy, University of Hawaii, Honolulu, HI 96822, USA*

⁸*Department of Physics, University of Wisconsin-Milwaukee, Milwaukee, WI 53201, USA*

⁹*Department of Physics and Astronomy, Vanderbilt University, Nashville TN 37235, USA*

(Dated: June 2015)

We study the vacuum stability of a minimal Higgs portal model in which the standard model (SM) particle spectrum is extended to include one complex scalar field and one Dirac fermion. These new fields are singlets under the SM gauge group and are charged under a global $U(1)$ symmetry. Breaking of this $U(1)$ symmetry results in a massless Goldstone boson, a massive CP -even scalar, and splits the Dirac fermion into two new mass-eigenstates, corresponding to Majorana fermions. The lightest Majorana fermion (w) is absolutely stable, providing a plausible dark matter (DM) candidate. We show that interactions between the Higgs sector and the lightest Majorana fermion which are strong enough to yield a thermal relic abundance consistent with observation can easily destabilize the electroweak vacuum or drive the theory into a non-perturbative regime at an energy scale well below the Planck mass. However, we also demonstrate that there is a region of the parameter space which develops a stable vacuum (up to the Planck scale), satisfies the relic abundance, and is in agreement with direct DM searches. Such an interesting region of the parameter space corresponds to DM masses $350 \text{ GeV} \lesssim m_w \lesssim 1 \text{ TeV}$. The region of interest is within reach of second generation DM direct detection experiments.

I. INTRODUCTION

The conspicuously well-known accomplishments of the $SU(3)_C \times SU(2)_L \times U(1)_Y$ standard model (SM) of strong and electroweak forces can be considered as the apotheosis of the gauge symmetry principle to describe particle interactions. Most spectacularly, the recent discovery [1, 2] of a new boson with scalar quantum numbers and couplings compatible with those of a SM Higgs has possibly plugged the final remaining experimental hole in the SM, cementing the theory further.

Arguably, the most challenging puzzle in high energy physics today is to find out what is the underlying theory that completes the SM. The overly conservative approach to this dilemma has been to assess the consistency of the SM assuming a vast desert between the electroweak scale $M_{\text{EW}} \sim 10^3 \text{ GeV}$ and the Planck mass $M_{\text{Pl}} \sim 10^{19} \text{ GeV}$. The relevant physics of the desert hypothesis is determined by running couplings into the ultraviolet (UV) using renormalization group (RG) equations. The behavior of the running couplings depends sensitively on the weak scale boundary conditions, among which the mass of the Higgs boson is perhaps the most critical. The measured Higgs mass $m_H = 125.5 \pm 0.5 \text{ GeV}$ [3–6] corresponds to a Higgs quartic coupling λ close to zero when renormalized at energies above $\Lambda \sim 10^{11} \text{ GeV}$.

Strictly speaking, next-to-leading order (NLO) constraints on SM vacuum stability based on two-loop RG equations, one-loop threshold corrections at the elec-

troweak scale (possibly improved with two-loop terms in the case of pure QCD corrections), and one-loop effective potential seem to indicate m_H saturates the minimum value that ensures a vanishing Higgs quartic coupling around M_{Pl} , see *e.g.* [7–17]. However, the devil is in the details. More recent NNLO analyses [18–20] yield a very restrictive condition of absolute stability up to the Planck scale

$$m_H > \left[129.4 + 1.4 \left(\frac{m_t/\text{GeV} - 173.1}{0.7} \right) - 0.5 \left(\frac{\alpha_s(m_Z) - 0.1184}{0.0007} \right) \pm 1.0_{\text{th}} \right] \text{ GeV}. \quad (1)$$

On combining in quadrature the theoretical uncertainty with experimental errors on the mass of the top (m_t) and the strong coupling constant (α_s), one obtains $m_H > 129 \pm 1.8 \text{ GeV}$. The vacuum stability of the SM up to the Planck scale is excluded at 2σ (98% C.L. one sided) for $m_H < 126 \text{ GeV}$ [18–20].

The instability of the SM vacuum does not contradict any experimental observation, provided its lifetime τ is longer than the age of the universe T_{U} . Since the stability condition of the electroweak vacuum is strongly sensitive to new physics, from the phenomenological point of view it is clear that beyond SM physics models have to pass a sort of “stability test” [21–23]. Indeed, only new physics models that reinforce the requirement of a stable or metastable (but with $\tau > T_{\text{U}}$) electroweak vacuum can be accepted as a viable UV completion of the SM [24–35].

From a theoretical perspective some modification of the Higgs sector has long been expected, as the major motivation for physics beyond the SM is aimed at resolving the huge disparity between the strength of gravity and of the SM forces. Even if one abandons this hierarchy motivation, which does not conflict with any experimental measurement, the SM has many other (perhaps more basic) shortcomings. Roughly speaking, the SM is incapable of explaining some well established observational results. Among the most notable of these are neutrino masses, the QCD theta parameter, and the presence of a large non-baryonic dark matter (DM) component of the energy density in the universe. Interestingly, if the new dynamics couples directly to the Higgs sector, this may induce deviations from the usual vacuum stability and perturbativity bounds of the SM. However, beyond SM physics models are usually driven by rather high scale dynamics (*e.g.*, the neutrino seesaw and the QCD axion), in which case there will be a negligible effect on the running of the couplings. A notable exception to this is the weakly interacting massive particle (WIMP) DM, whose mass scale is constrained to be low if produced by thermal freeze-out [36].

The scalar Higgs portal is a compelling model of WIMP DM in which a renormalizable coupling with the Higgs boson provides the connection between our visible world and a dark sector consisting of $SU(3)_C \times SU(2)_L \times U(1)_Y$ singlet fields [37–40]. This is possible because the Higgs bilinear $\Phi^\dagger \Phi$ is the only dimension-2 operator of the SM that is gauge and Lorentz invariant, allowing for an interaction term with a complex singlet scalar S of the form

$$\Delta V = \lambda_3 \Phi^\dagger \Phi S^\dagger S. \quad (2)$$

Given that S develops a vacuum expectation value (VEV), the Higgs mixes with the singlet leading to the existence of two mass eigenstates (h_1 and h_2), which in turn open the portal into a weak scale hidden sector. Despite its simplicity, in fact, this model offers a rich phenomenology, and it provides a simple and motivated paradigm of DM.

In this paper we carry out a general analysis of vacuum stability and perturbativity in the SM augmented by a Higgs portal with a minimal weak scale hidden sector. The layout is as follows. In Sec. II we outline the basic setting of the scalar Higgs portal model and discuss general aspects of the effective low energy theory resulting from a minimal hidden sector. In Sec. III we confront the model with a variety of experimental data, including direct DM searches, heavy meson decays with missing energy, the invisible Higgs width, as well as astrophysical and cosmological observations. In Sec. IV we derive the RG equations and in Sec. V we present the analysis of vacuum stability. Our conclusions are collected in Sec. VI.

II. MINIMAL HIGGS PORTAL MODEL

A viable DM candidate must be stable, or nearly so. Stability results from either an unbroken or mildly broken symmetry in the Lagrangian. A discrete Z_2 symmetry is the simplest available symmetry to guarantee absolute stability of the DM particle. Under Z_2 the SM particles are even while the DM particle is odd [41]. The required symmetry may be simply introduced by hand into the SM, or, more naturally, may remain after breaking of some global continuous symmetry. For example, a concrete realization of such a hidden sector could emerge when a global $U(1)$ symmetry is spontaneously broken by a scalar field with charge 2 under that symmetry, and so a discrete Z_2 symmetry arises automatically in the Lagrangian. After spontaneous symmetry breaking, fields with an even (odd) charge under the global $U(1)$ symmetry will acquire an even (odd) discrete charge under Z_2 . Consequently the lightest particle with odd charge will be absolutely stable, and thus a plausible dark matter candidate. The simplest approach to realize this scenario is to introduce one new complex scalar field S and one Dirac fermion field ψ into the SM. These new fields are singlets under the SM gauge group, and charged under $U(1)_W$ symmetry, such that $U(1)_W(\psi) = 1$ and $U(1)_W(S) = 2$. Spontaneous breaking of a global continuous symmetry generates a massless Goldstone boson and a CP -even scalar, and splits the Dirac fermion into two new mass-eigenstates, corresponding to Majorana fermions.

The renormalizable scalar Lagrangian density of the set up described above is found to be

$$\mathcal{L}_s = (\mathcal{D}^\mu \Phi)^\dagger \mathcal{D}_\mu \Phi + (\mathcal{D}^\mu S)^\dagger \mathcal{D}_\mu S - V, \quad (3)$$

where

$$V = \mu_1^2 \Phi^\dagger \Phi + \mu_2^2 S^\dagger S + \lambda_1 (\Phi^\dagger \Phi)^2 + \lambda_2 (S^\dagger S)^2 + \Delta V \quad (4)$$

is the potential and

$$\mathcal{D}_\mu = \partial_\mu - ig_2 \tau^a W_\mu^a - ig_Y Y B_\mu \quad (5)$$

is (in a self-explanatory notation) the covariant derivative. In the spirit of [42], we write S in terms of two real fields (its massive radial component and a massless Goldstone boson). The radial field develops a VEV $\langle r \rangle$ about which the field S is expanded

$$S = \frac{1}{\sqrt{2}} (\langle r \rangle + r(x)) e^{i 2\alpha(x)}. \quad (6)$$

The phase of S is adjusted to make $\langle \alpha(x) \rangle = 0$. Next, we impose the positivity conditions [40]

$$\lambda_1 > 0, \quad \lambda_2 > 0, \quad \lambda_1 \lambda_2 > \frac{1}{4} \lambda_3^2. \quad (7)$$

If the conditions (7) are satisfied, we can proceed to the minimization of (4) as a function of constant VEVs for

the two scalar fields. In the unitary gauge the Higgs doublet is expanded around the VEV as

$$\Phi(x) = \frac{1}{\sqrt{2}} \begin{pmatrix} 0 \\ \langle \phi \rangle + \phi(x) \end{pmatrix}, \quad (8)$$

where $\langle \phi \rangle = 246$ GeV.

The physically most interesting solutions to the minimization of (4) are obtained for $\langle \phi \rangle$ and $\langle r \rangle$ both non-vanishing

$$\langle \phi \rangle^2 = \frac{-\lambda_2 \mu_1^2 + \frac{1}{2} \lambda_3 \mu_2^2}{\lambda_1 \lambda_2 - \frac{1}{4} \lambda_3^2} \quad (9)$$

and

$$\langle r \rangle^2 = \frac{-\lambda_1 \mu_2^2 + \frac{1}{2} \lambda_3 \mu_1^2}{\lambda_1 \lambda_2 - \frac{1}{4} \lambda_3^2}. \quad (10)$$

To compute the scalar masses, we must expand the potential (4) around the minima (9) and (10). We denote by h_1 and h_2 the scalar fields of definite masses, m_{h_1} and m_{h_2} respectively. After a bit of algebra, the explicit expressions for the scalar mass eigenvalues and eigenvectors read

$$m_{h_1}^2 = \lambda_1 \langle \phi \rangle^2 + \lambda_2 \langle r \rangle^2 - \zeta, \quad (11)$$

and

$$m_{h_2}^2 = \lambda_1 \langle \phi \rangle^2 + \lambda_2 \langle r \rangle^2 + \zeta, \quad (12)$$

with

$$\zeta = \sqrt{(\lambda_1 \langle \phi \rangle^2 - \lambda_2 \langle r \rangle^2)^2 + (\lambda_3 \langle \phi \rangle \langle r \rangle)^2} \quad (13)$$

and

$$\begin{pmatrix} h_1 \\ h_2 \end{pmatrix} = \begin{pmatrix} \cos \theta & -\sin \theta \\ \sin \theta & \cos \theta \end{pmatrix} \begin{pmatrix} r \\ \phi \end{pmatrix}. \quad (14)$$

Here, $\theta \in [-\pi/2, \pi/2]$ also fullfills

$$\sin 2\theta = \frac{\lambda_3 \langle \phi \rangle \langle r \rangle}{\sqrt{(\lambda_1 \langle \phi \rangle^2 - \lambda_2 \langle r \rangle^2)^2 + (\lambda_3 \langle \phi \rangle \langle r \rangle)^2}}. \quad (15)$$

Now, it is convenient to invert (11), (12) and (15), to extract the parameters in the Lagrangian in terms of measurable quantities: m_{h_1} , m_{h_2} and $\sin 2\theta$. We obtain

$$\begin{aligned} \lambda_1 &= \frac{m_{h_2,1}^2}{4\langle \phi \rangle^2} (1 - \cos 2\theta) + \frac{m_{h_1,2}^2}{4\langle \phi \rangle^2} (1 + \cos 2\theta), \\ \lambda_2 &= \frac{m_{h_1,2}^2}{4\langle r \rangle^2} (1 - \cos 2\theta) + \frac{m_{h_2,1}^2}{4\langle r \rangle^2} (1 + \cos 2\theta), \\ \lambda_3 &= \sin 2\theta \left(\frac{m_{h_2,1}^2 - m_{h_1,2}^2}{2\langle \phi \rangle \langle r \rangle} \right). \end{aligned} \quad (16)$$

Note that there are two distinct regions of the parameter space: one in which the hidden scalar singlet is heavier

than the Higgs doublet and one in which is lighter. The small θ limit leads to the usual SM phenomenology with an isolated hidden sector.

For the DM sector we assume at least one Dirac field

$$\mathcal{L}_\psi = i\bar{\psi}\gamma \cdot \partial\psi - m_\psi \bar{\psi}\psi - \frac{f}{\sqrt{2}} \bar{\psi}^c \psi S^\dagger - \frac{f^*}{\sqrt{2}} \bar{\psi} \psi^c S. \quad (17)$$

As advanced above, we assign to the hidden fermion a charge $U(1)_W(\psi) = 1$, so that the Lagrangian is invariant under the global transformation $e^{iW\alpha}$. Assuming the transformation is local we express ψ as

$$\psi(x) = \psi'(x) e^{i\alpha(x)}. \quad (18)$$

Now, after r achieves a VEV we expand the DM sector to obtain

$$\begin{aligned} \mathcal{L}_\psi &= \frac{i}{2} \left(\bar{\psi}' \gamma \cdot \partial\psi' + \bar{\psi}'^c \gamma \cdot \partial\psi'^c \right), \\ &- \frac{m_\psi}{2} (\bar{\psi}' \psi' + \bar{\psi}'^c \psi'^c) - \frac{f\langle r \rangle}{2} \bar{\psi}'^c \psi' - \frac{f\langle r \rangle}{2} \bar{\psi}' \psi'^c, \\ &- \frac{1}{2} (\bar{\psi}' \gamma \psi' - \bar{\psi}'^c \gamma \psi'^c) \cdot \partial\alpha, \\ &- \frac{f}{2} r (\bar{\psi}'^c \psi' + \bar{\psi}' \psi'^c). \end{aligned} \quad (19)$$

The diagonalization of the ψ' mass matrix generates the mass eigenvalues,

$$m_\pm = m_\psi \pm f\langle r \rangle, \quad (20)$$

for the two mass eigenstates

$$\psi_- = \frac{i}{\sqrt{2}} (\psi'^c - \psi') \quad \text{and} \quad \psi_+ = \frac{1}{\sqrt{2}} (\psi'^c + \psi'). \quad (21)$$

In the new basis, the act of charge conjugation on ψ_\pm yields

$$\psi_\pm^c = \psi_\pm, \quad (22)$$

which implies that the fields ψ_\pm are Majorana fermions. The Lagrangian is found to be

$$\begin{aligned} \mathcal{L}_\psi &= \frac{i}{2} \bar{\psi}_+ \gamma \cdot \partial\psi_+ + \frac{i}{2} \bar{\psi}_- \gamma \cdot \partial\psi_- \\ &- \frac{1}{2} m_+ \bar{\psi}_+ \psi_+ - \frac{1}{2} m_- \bar{\psi}_- \psi_-, \\ &- \frac{i}{4\langle r \rangle} (\bar{\psi}_+ \gamma \psi_- + \bar{\psi}_- \gamma \psi_+) \cdot \partial\alpha', \\ &- \frac{f}{2} r (\bar{\psi}_+ \psi_+ + \bar{\psi}_- \psi_-), \end{aligned} \quad (23)$$

where $\alpha' \equiv 2\alpha\langle r \rangle$ is the canonically normalized Goldstone boson [42]. We must now put r into its massive field representation, for which the interactions of interest are

$$\begin{aligned} \mathcal{L} &= -\frac{f \sin \theta}{2} h_{1,2} (\bar{\psi}_+ \psi_+ + \bar{\psi}_- \psi_-) - \frac{f \cos \theta}{2} h_{2,1} \\ &\times (\bar{\psi}_+ \psi_+ + \bar{\psi}_- \psi_-). \end{aligned} \quad (24)$$

TABLE I. Definition of most common variables.

Φ	Higgs doublet
S	Complex scalar field
ϕ	Neutral component of Φ
r	Massive CP -even scalar
α'	Goldstone boson
H	SM Higgs boson
$h_{1,2}$	Scalar mass eigenstates
λ_3	Quartic coupling between SM and hidden sector
θ	Mixing angle between h_1 and h_2
w	Lightest Majorana fermion (WIMP)
f	$w - r$ coupling constant – see Eq. (23) –

This leads to 3-point interactions between the Majorana fermions and the Higgs doublet.

All in all, the Dirac fermion of the hidden sector splits into two Majorana mass-eigenstates. The heavier state will decay into the lighter one by emitting a Goldstone boson. The lighter one, however, is kept stable by the unbroken reflection symmetry. Hence, we can predict that today the universe will contain only one species of Majorana WIMP, the lighter one w , with mass m_w equal to the smaller of m_{\pm} . Therefore, the dark sector contains five unknown parameters: m_w , $m_{h_{1,2}}$, λ_2 , θ , and f . To facilitate the calculation of the WIMP relic density, throughout we impose a supplementary constraint relating some of these free parameters: $\Delta m/m_w \ll 1$, where $\Delta m = |m_+ - m_-| = 2|f\langle r \rangle|$. (The most common variables used in this article are summarized in Table I.)

A cautionary note is worth taking on board at this juncture. It is well known that the spontaneous breaking of a global $U(1)$ symmetry have several disconnected and degenerate vacua (the phase of the vacuum expectation value $\langle 0|S|0 \rangle$ can be different in different regions of space, and actually we expect it to be different in causally disconnected regions), yielding dangerous domain-wall structure in the early universe [43, 44]. In the spirit of [43], it may be possible to explicitly break the symmetry introducing (possibly small) terms in V , such that the domain walls disappear before dominating the matter density of the universe, while leaving (pseudo-)Goldstone bosons and the same dark matter phenomenology [26].¹ For simplicity, we restrict our considerations to the potential in (4), but generalizations are straightforward.

III. CONSTRAINTS FROM EXPERIMENT

The mixing of r with the Higgs doublet ϕ can be analyzed in a two-parameter space characterized by the mass of hidden scalar m_{h_i} and the mixing angle θ , where $i = 1$ for a light scalar singlet (*i.e.* $m_{h_2} = m_H$) and $i = 2$ for

a heavy one (*i.e.* $m_{h_1} = m_H$). We begin to constrain this parameter space by using data from DM searches at direct detection experiments.

A. Constraints from direct DM searches

The wN cross section for elastic scattering is found to be

$$\sigma_{wN} = \frac{4}{\pi} \frac{m_w^2 m_N^2}{(m_w + m_N)^2} \frac{f_p^2 + f_n^2}{2}, \quad (25)$$

where $N \equiv \frac{1}{2}(n + p)$ is an isoscalar nucleon in the renormalization group-improved parton model [48, 49]. The effective couplings to protons f_p and neutrons f_n are given by

$$f_{p,n} = \sum_{q=u,d,s} \frac{G_q}{\sqrt{2}} f_{S_q}^{(p,n)} \frac{m_{p,n}}{m_q} + \frac{2}{27} f_{SG}^{(p,n)} \times \sum_{q=c,b,t} \frac{G_q}{\sqrt{2}} \frac{m_{p,n}}{m_q}, \quad (26)$$

where G_q is the WIMP's effective Fermi coupling for a given quark species,

$$\mathcal{L} = \frac{G_q}{\sqrt{2}} \bar{\psi}_- \psi_- \bar{\psi}_q \psi_q, \quad (27)$$

with ψ_q the SM quark field of flavor q . The first term in (26) reflects scattering with light quarks, whereas the second term accounts for interaction with gluons through a heavy quark loop. The scalar spin-independent form factors, $f_{S_q}^{(p,n)}$, are proportional to the matrix element, $\langle \bar{q}q \rangle$, of quarks in a nucleon. Herein we take [50]

$$\begin{aligned} f_{S_u}^p &= 0.016(5)(3)(1), & f_{S_u}^n &= 0.014(5)(\begin{smallmatrix} +2 \\ -3 \end{smallmatrix})(1), \\ f_{S_d}^p &= 0.029(9)(3)(2), & f_{S_d}^n &= 0.034(9)(\begin{smallmatrix} +3 \\ -2 \end{smallmatrix})(2), \\ f_{S_s}^p &= 0.043(21), & f_{S_s}^n &= 0.043(21), \end{aligned} \quad (28)$$

in good agreement with the scalar strange content of the nucleon from lattice QCD calculations [51]. The gluon scalar form factor is given by $f_{SG}^{(p,n)} = 1 - \sum_{u,d,s} f_{S_q}^{(p,n)}$. For the case at hand,

$$\frac{f_p^2 + f_n^2}{2m_N^2} \simeq \left(0.29 \frac{G_q}{\sqrt{2}m_q} \right)^2, \quad (29)$$

with

$$\frac{G_q}{m_q} = \frac{\sqrt{2}f\lambda_3\langle r \rangle}{2m_{h_1}^2 m_{h_2}^2}, \quad (30)$$

yielding [52]

$$\sigma_{wN} = \frac{1}{\pi} \frac{m_w^2 m_N^4}{(m_w + m_N)^2} \left(\frac{0.29 \lambda_3 \langle r \rangle f}{m_{h_1}^2 m_{h_2}^2} \right)^2; \quad (31)$$

¹ Other approaches, if exceedingly fine-tuned, may offer alternative solutions [45–47].

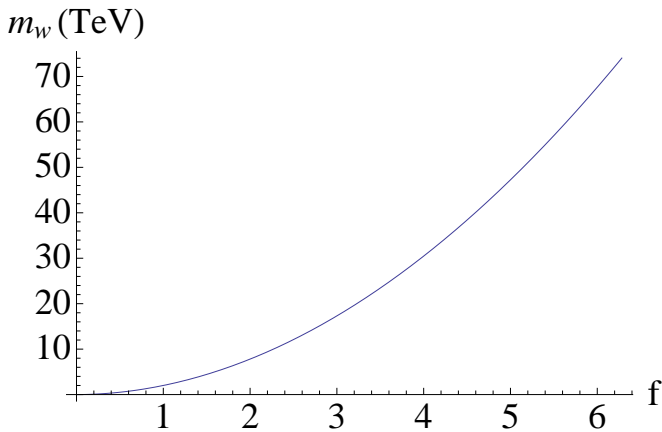


FIG. 1. The relation in Eq. (35).

see Appendix A for details. We may re-express this result in terms of the mixing angle,

$$\sigma_{wN} = (0.29)^2 \frac{1}{4\pi} \frac{m_w^2 m_N^4}{(m_w + m_N)^2} \left(\frac{1}{m_{h_1}^2} - \frac{1}{m_{h_2}^2} \right)^2 \times \left(\frac{f}{\langle \phi \rangle} \right)^2 \sin^2 2\theta. \quad (32)$$

For $\theta \ll 1$, the upper limits on the nucleon-wimp cross sections derived by the various experiments translate into upper limits on the mixing angle

$$|\theta| < \frac{(m_w + m_N) \langle \phi \rangle}{m_N^2 m_w} \frac{1}{f} \left| \frac{1}{m_{h_1}^2} - \frac{1}{m_{h_2}^2} \right|^{-1} \times \frac{\sqrt{\pi}}{0.29} \sqrt{\sigma_{wN}(m_w)}. \quad (33)$$

To determine f we require the w relic density to be consistent with $h^2 \Omega_{\text{DM}} \simeq 0.111(6)$ [53]. In our study we consider the interesting case in which $m_{h_i} < m_w$ and hence the instantaneous freeze-out approximation is valid [54]. In this region of the parameter space, the w 's predominantly annihilate into a pair of h_i 's or co-annihilate with the next-to-lightest Majorana fermion, producing a scalar h_i and a Goldstone boson. All of the final state h_i subsequently decays into α' . We note, however, that for $m_w \approx m_H/2$ one expects dominant annihilation into fermions. We have found that for the considerations in the present work, the effective thermal cross section can be safely approximated by [54]

$$\lim_{\Delta m/m_w \rightarrow 0} \langle \sigma_{ww} v_M \rangle \approx \frac{f^4}{32\pi m_w^2}, \quad (34)$$

yielding

$$f \approx \left(\frac{1.04 \times 10^{11} \text{ GeV}^{-1} x_f}{\sqrt{g(x_f)} M_{\text{Pl}} \Omega_{\text{DM}} h^2} \right)^{1/4} \sqrt{m_w}, \quad (35)$$

where $x_f = m_w/T_f$, $g(x_f)$ is the number of relativistic degrees of freedom at the freeze-out temperature T_f , and $m_{h_i}/m_w \lesssim 0.8$ [54]. In general for WIMP DM $x_f \approx 20 - 25$ [55]. The precise relation between the WIMP mass and the required Yukawa coupling to attain the relic density condition is shown in Fig. 1. We note that the mass upper limit, $m_w < 74$ TeV, is in agreement with the unitarity limit $\Omega_{\text{DM}} h^2 \geq 1.7 \times 10^{-6} \sqrt{x_f} [m_w/(1 \text{ TeV})]^2$ [56], which implies $m_w \leq 110$ TeV [57].

Using (33) we can now translate the 90% confidence limit on the spin independent elastic WIMP-nucleon cross section as obtained by direct detection experiments into an upper limit of $|\theta|$. In Fig. 2 we show constraints on this parameter space from direct dark matter searches. For $m_w \gtrsim 8$ GeV, the most restrictive constraint comes from the LUX experiment [58], whereas for $m_w \lesssim 8$ GeV, the most restrictive upper limit is from the SuperCDMS low threshold experiment [59]. It should be noted that indirect DM searches (*e.g.* by detecting neutrinos from annihilation of captured low-mass WIMPs in the Sun) also constrain the WIMP-nucleon elastic scattering cross section. However, these searches are in general model dependent. For example, for 100% annihilation into $\tau^+ \tau^-$ pairs, the Super-Kamiokande Collaboration [60] has set the current best upper limit on σ_{wN} for WIMP masses below 8 GeV. Because of the assumed dominant decay into SM fields, this limit cannot be used to further constrain the (θ, m_h) parameter space.

B. Constraints from heavy meson decay

For $m_w \lesssim 10$ GeV, searches for heavy meson decays with missing energy provide comparable bounds [61–63]. In particular, the upper limit reported by the BaBar Collaboration $\mathcal{B}(\Upsilon(1S) \rightarrow \gamma + \cancel{E}_T) < 2 \times 10^{-6}$ [64] yields an upper bound for the mixing angle, $\theta < 0.27$ [65].² A stronger constraint follows from LEP limits on the production of invisibly-decaying Higgs bosons $\sigma_{Zh}/\sigma_{ZH} < 10^{-4}$ [68–72], which implies $\theta < 10^{-2}$ [73]. More restrictive constraints come from searches for the rare flavor-changing neutral-current decay $B^+ \rightarrow K^+ + \cancel{E}_T$ reported by the BaBar [74–76], CLEO [77], and BELLE [78] collaborations, as well as limits on $K^+ \rightarrow \pi^+ + \cancel{E}_T$ from the E787 [79] and E949 experiments [80–82]. The resulting excluded regions of the $(|\theta|, m_h)$ plane from all these experiments are compared in Fig. 2 with those from direct DM searches.

C. Constraints from LHC and SN1987A

Before proceeding we note that additional constraints on the $(|\theta|, m_h)$ parameter space can be obtained from

² Comparable bounds are obtained from searches for $\mathcal{B}(\Upsilon(3S) \rightarrow \gamma + \cancel{E}_T)$ [66] and $\mathcal{B}(J/\psi \rightarrow \gamma + \cancel{E}_T)$ [67].

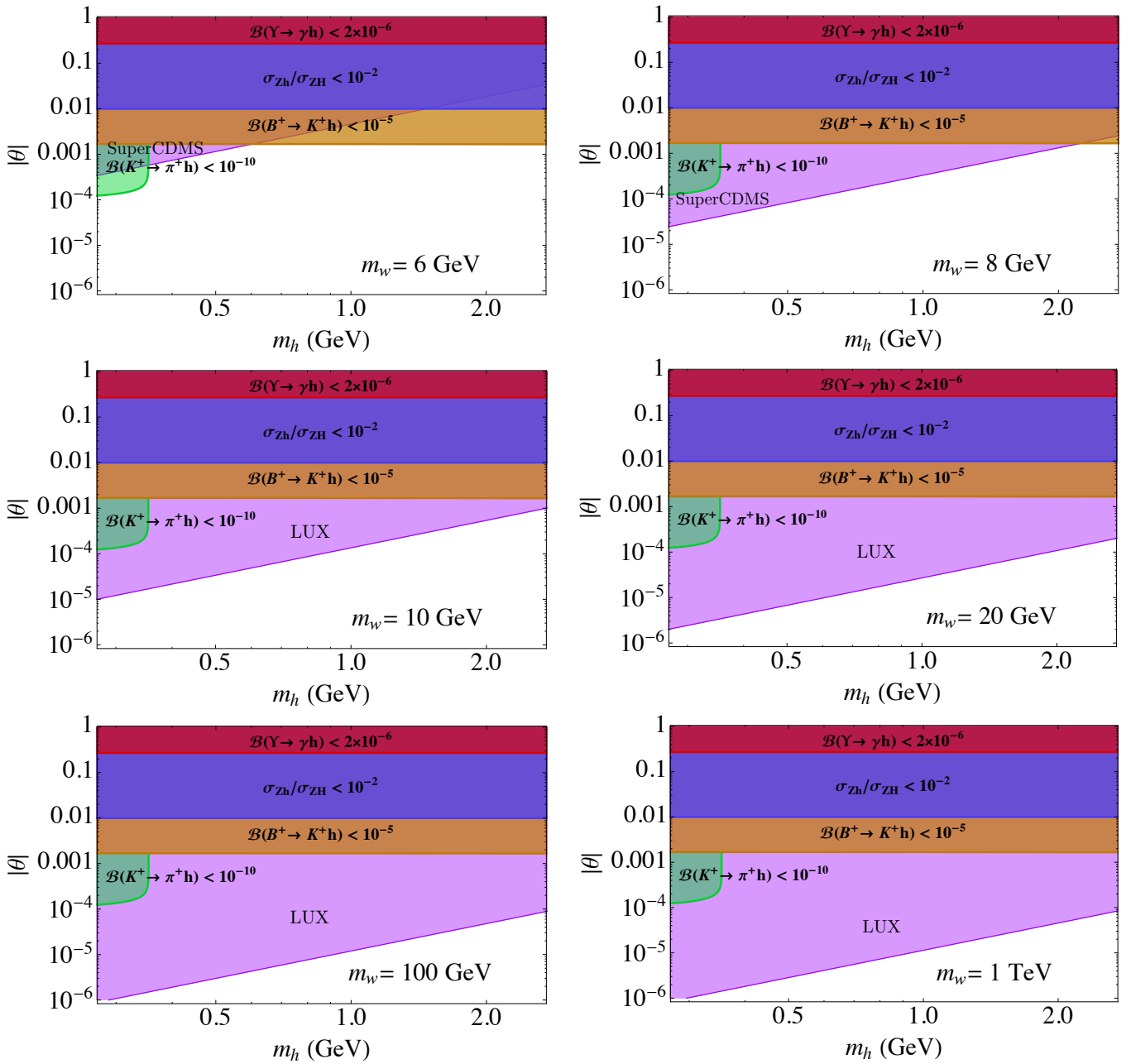


FIG. 2. Excluded regions of the $(|\theta|, m_h)$ parameter space from interactions involving SM particles in the initial state and the CP -even scalar in the final state, as well from DM direct detection experiments. The horizontal bands indicate bounds are from heavy meson decays with missing energy (no significant excess of such decays over background has been observed yielding bounds on the processes $\Upsilon \rightarrow \gamma h$, $B^+ \rightarrow K^+ h$, $K^+ \rightarrow \pi^+ h$) as well as from LEP limits on the production of invisibly-decaying Higgs bosons σ_{Zh}/σ_{ZH} . The diagonal bands represent bounds from DM direct detection experiments (Super-CDMS and LUX), for different values of the WIMP mass. Note that all bounds other than the LEP bound can be smoothly extrapolated to the smallest $m_h \sim 35$ MeV stipulated by cosmology.

limits on Higgs decay into invisible particles and from emission of α' -particle pairs in a post-collapse supernova core. However, these are not direct constraints as they depend also on the quartic coupling of the hidden scalar. In particular, since invisible decays reduce the branching fraction to the (visible) SM final states, it is to be expected that $\mathcal{B}(H \rightarrow \text{invisible})$ is strongly constrained.

Indeed $\mathcal{B}(H \rightarrow \text{invisible})$ is known to be less than about 19% at 95%CL [83–87]. This implies exclusion contours in the $(|\theta|, m_h)$ plane as a function of the free parameter

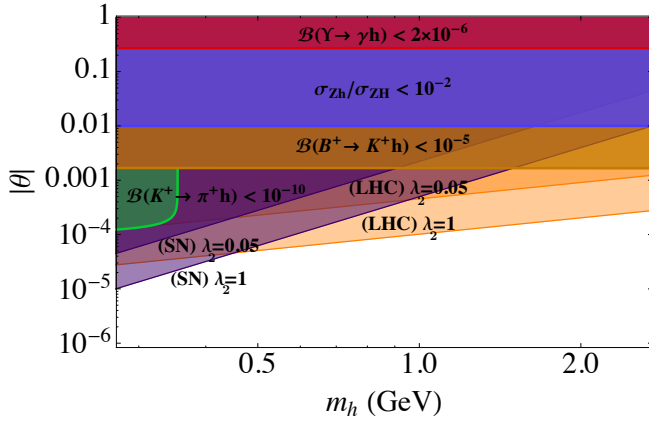


FIG. 3. Bounds on the $(|\theta|, m_h)$ including invisible Higgs decays and α' emission in a post-collapse supernova core for different assumptions about the value of the quartic coupling λ_2 .

λ_2 given by [63]

$$|\theta(\lambda_2)| < 1.27 \times 10^{-2} \left[\lambda_2 \frac{m_H^2}{m_h^2} + f^2 \sqrt{1 - \frac{4m_w^2}{m_H^2}} \right]^{-\frac{1}{2}}.$$

In addition, the emissivity of α' due to nucleon bremsstrahlung ($NN \rightarrow NN\alpha'\alpha'$) cannot exceed the limits imposed by SN1987A observations: $\epsilon_{\alpha'} \leq 7.324 \times 10^{-27}$ GeV [88]. For typical supernova core conditions ($T = 30$ MeV and $\rho = 3 \times 10^{14}$ g/cm³) it is easily seen that $|\lambda_3| \leq 0.011 \left(\frac{m_h}{500 \text{ MeV}}\right)^2$ [89]. For $\theta \ll 1$ we can translate this limit into a bound on the mixing angle via

$$\theta \approx \frac{\lambda_3 \langle r \rangle \langle \phi \rangle}{m_H^2 - m_h^2}. \quad (36)$$

By use of $m_h \approx \sqrt{2\lambda_2} \langle r \rangle$ we can express this bound as

$$|\theta| \leq \frac{7.65 m_h^3}{\sqrt{\lambda_2} |m_H^2 - m_h^2|} \text{ GeV}^{-1}. \quad (37)$$

In Fig. 3 we show the exclusion contours for the $\lambda_2 = 1$ and $\lambda_2 = 0.05$. For smaller values of λ_2 , the excluded regions of the $(|\theta|, m_h)$ plane are dominated by upper limits on B -meson decay into invisibles. All in all, for $m_{h_2} = m_H$, we can conclude from Figs. 2 and 3 that 2×10^{-3} is a conservative 90% CL upper limit on the mixing angle.

For $m_{h_2} \gg m_H$, (33) can be rewritten as

$$f |\theta| < \frac{1}{m_N^2} \langle \phi \rangle m_H^2 \frac{\sqrt{\pi}}{0.29} \sqrt{\sigma_w N(m_w)} \\ \simeq 2.7 \times 10^7 \sqrt{\sigma_w N(m_w)} \text{ GeV}. \quad (38)$$

Dedicated searches for DM candidates serve as an essential component of the LHC physics programme. The typical experimental signature of DM production at the

LHC consists of an excess of events with a single final-state particle X recoiling against large amounts of missing transverse momentum or energy. In Run I, the ATLAS and CMS collaborations have examined a variety of such “mono- X ” topologies involving jets of hadrons, gauge bosons, top and bottom quarks as well as the Higgs boson in the final state. In particular, the CMS Collaboration has reported very restrictive bounds on the DM-nucleon scattering cross section from searches in events containing a jet and an imbalanced transverse momentum [90]. However, it is important to stress that the contact operator approximation adopted in [90] only holds if the mediator is heavy and can be integrated out [91]. If the mediator is light and contributes to resonant DM production (as in the minimal Higgs portal model discussed herein), the contact approximation fails and the mono-jet bounds do not apply. Future LHC14 mono- X searches will also probe vertex operators for which the mediator between dark matter and quarks is heavy [92, 93], and therefore cannot constrain the Higgs portal model discussed in this paper.

D. Constraints from cosmology

Cosmological observations further constrain the model. The earliest observationally verified landmarks – big bang nucleosynthesis (BBN) and the cosmic microwave background (CMB) decoupling epoch – have become the de facto worldwide standard for probing theoretical scenarios beyond the SM containing new light species. It is advantageous to normalize the extra contribution to the SM energy density to that of an “equivalent” neutrino species. The number of “equivalent” light neutrino species,

$$N_{\text{eff}} = \frac{\rho_{\text{R}} - \rho_{\gamma}}{\rho_{\nu_L}}, \quad (39)$$

quantifies the total “dark” relativistic energy density (including the three left-handed SM neutrinos) in units of the density of a single Weyl neutrino

$$\rho_{\nu_L} = \frac{7\pi^2}{120} \left(\frac{4}{11}\right)^{4/3} T_{\gamma}^4, \quad (40)$$

where ρ_{γ} is the energy density of photons (which by today have redshifted to become the CMB photons at a temperature of about $T_{\gamma}^{\text{today}} \simeq 2.7$ K) [94].

Recent results reported by the Planck Collaboration [95] have strongly constrained the presence of an excess ΔN_{eff} above SM expectation: $N_{\text{eff}}^{\text{SM}} = 3.046$ [96]. Specifically, the 68% C.L. constraints on N_{eff} from Planck TT, TE, and EE spectra, when combined with polarization maps (lowP) and baryon acoustic oscillation (BAO) measurements are [95]:

$$N_{\text{eff}} = \begin{cases} 3.13 \pm 0.32 & \text{PlanckTT + lowP,} \\ 3.15 \pm 0.23 & \text{PlanckTT + lowP + BAO,} \\ 2.99 \pm 0.20 & \text{PlanckTT, TE, EE + lowP,} \\ 3.04 \pm 0.18 & \text{PlanckTT, TE, EE + lowP + BAO.} \end{cases}$$

The joint CMB+BBN predictions on N_{eff} provide comparable constraints. The 95% C.L. preferred range on N_{eff} when combining Planck data (TT, TE, EE+lowP) with the helium abundance estimated in [97] is $N_{\text{eff}} = 2.99 \pm 0.39$, whereas the combination of Planck data with the deuterium abundance measured in [98] yields $N_{\text{eff}} = 2.91 \pm 0.37$ [95]. (See also [99].) In summary, one fully thermalize neutrino, $\Delta N_{\text{eff}} \simeq 1$, is excluded at over 3σ . Models predicting fractional changes of $\Delta N_{\text{eff}} \approx 0.39$ are marginally consistent with data, saturating the 1σ upper limit. Models predicting, $\Delta N_{\text{eff}} \approx 0.57$, are ruled out at about 2σ .

As noted in [42] the Goldstone boson α' is a natural candidate for an imposter equivalent neutrino. The contribution of α' to N_{eff} is $\Delta N_{\text{eff}} = \rho_{\alpha'}/\rho_\nu$. Thus, taking into account the isentropic heating of the rest of the plasma between the decoupling temperatures, $T_{\alpha'}^{\text{dec}}$ and T_ν^{dec} , we obtain

$$\Delta N_{\text{eff}} = \frac{4}{7} \left(\frac{g(T_\nu^{\text{dec}})}{g(T_{\alpha'}^{\text{dec}})} \right)^{4/3}, \quad (41)$$

where $g(T)$ is the effective number of interacting (thermally coupled) relativistic degrees of freedom at temperature T ; for example, $g(T_\nu^{\text{dec}}) = 43/4$.³ For the particle content of the SM, there is a maximum of $g(T_{\alpha'}^{\text{dec}}) = 427/4$ (with $T_{\alpha'}^{\text{dec}} > m_t$). This corresponds to a minimum value of $\Delta N_{\text{eff}} = 0.027$, which is consistent with cosmological observations. However, a fully thermalized α' , *i.e.* $T_\nu^{\text{dec}} = T_{\alpha'}^{\text{dec}}$ is excluded at 90% C.L.. Note that if α' goes out of thermal equilibrium while the temperature is just above the muon mass

$$\Delta N_{\text{eff}} = (4/7)(43/57)^{4/3} = 0.39. \quad (42)$$

This corresponds to a number of equivalent light neutrino species that is consistent at the 1σ level with current data.

The α' decouples from the plasma when its mean free path becomes greater than the Hubble radius at that time. The α' collision rate with any fermion species of mass m_f at or below T is of order [42]

$$\Gamma(T) \sim \frac{\lambda_3^2 m_f^2 T^7}{m_{h_1}^4 m_{h_2}^4}, \quad (43)$$

whereas the expansion rate of the universe is of order

$$H(T) \approx \frac{T^2}{M_{\text{Pl}}}. \quad (44)$$

We equate these two rates to obtain

$$T_{\alpha'}^{\text{dec}} \approx \left(\frac{m_{h_1}^2 m_{h_2}^2}{\lambda_3 m_f M_{\text{Pl}}} \right)^{1/5}. \quad (45)$$

Now, taking $m_f = T = m_\mu$ we obtain

$$m_h \approx \frac{(\lambda_3^2 m_\mu^7 M_{\text{Pl}})^{1/4}}{m_H^4}. \quad (46)$$

Substituting the conservative value $\lambda_3 = 5 \times 10^{-3}$ in (46) we have $m_h \approx 500$ MeV. Note that if the α' goes out of equilibrium when the only massive SM particles left are e^+e^- pairs, $\Delta N_{\text{eff}} = 0.57$. In such a case the value of m_h would have to be less than given by (46) by a factor between $(m_e/m_\mu)^{1/2}$ and $(m_e/m_\mu)^{7/4}$ [42]. This sets a lower limit on the mass of the hidden scalar: $m_h \approx 35$ MeV.

IV. RG EVOLUTION EQUATIONS

One-loop corrections to (4) can be implemented by making λ_1 , λ_2 , and λ_3 energy dependent quantities. The positivity conditions of (7) then must be satisfied at all energies.

A straightforward calculation leads to the RG equations for the five parameters in the scalar potential

$$\begin{aligned} \frac{d\mu_1^2}{dt} &= \frac{\mu_1^2}{16\pi^2} \left(12\lambda_1 + 6Y_t^2 + 2\frac{\mu_2^2}{\mu_1^2}\lambda_3 - \frac{9}{2}g_2^2 - \frac{3}{2}g_Y^2 \right), \\ \frac{d\mu_2^2}{dt} &= \frac{\mu_2^2}{16\pi^2} \left(8\lambda_2 + 4\frac{\mu_1^2}{\mu_2^2}\lambda_3 + 4f^2 \right), \\ \frac{d\lambda_1}{dt} &= \frac{1}{16\pi^2} \left(24\lambda_1^2 + \lambda_3^2 - 6Y_t^4 + \frac{9}{8}g_2^4 + \frac{3}{8}g_Y^4 \right. \\ &\quad \left. + \frac{3}{4}g_2^2g_Y^2 + 12\lambda_1Y_t^2 - 9\lambda_1g_2^2 - 3\lambda_1g_Y^2 \right), \\ \frac{d\lambda_2}{dt} &= \frac{1}{8\pi^2} \left(10\lambda_2^2 + \lambda_3^2 - \frac{1}{4}f^4 + 4\lambda_2f^2 \right), \\ \frac{d\lambda_3}{dt} &= \frac{\lambda_3}{8\pi^2} \left(6\lambda_1 + 4\lambda_2 + 2\lambda_3 + 3Y_t^2 - \frac{9}{4}g_2^2 \right. \\ &\quad \left. - \frac{3}{4}g_Y^2 + 2f^2 \right), \end{aligned} \quad (47)$$

where $t = \ln Q$ and Y_t is the top Yukawa coupling, with

$$\frac{dY_t}{dt} = \frac{Y_t}{16\pi^2} \left(\frac{9}{2}Y_t^2 - 8g_3^2 - \frac{9}{4}g_2^2 - \frac{17}{12}g_Y^2 \right), \quad (48)$$

and $Y_t^{(0)} = \sqrt{2} m_t / \langle \phi \rangle$ (see Appendix B for details). The RG running of the gauge couplings follow the standard

³ If relativistic particles are present that have decoupled from the photons, it is necessary to distinguish between two kinds of g : g_ρ , which is associated with the total energy density, and g_s , which is associated with the total entropy density. For our calculations we use $g = g_\rho = g_s$.

form

$$\begin{aligned}\frac{dg_3}{dt} &= \frac{g_3^3}{16\pi^2} \left[-11 + \frac{4}{3}n_g \right] = -\frac{7}{16} \frac{g_3^3}{\pi^2}, \\ \frac{dg_2}{dt} &= \frac{g_2^3}{16\pi^2} \left[-\frac{22}{3} + \frac{4}{3}n_g + \frac{1}{6} \right] = -\frac{19}{96} \frac{g_2^3}{\pi^2}, \\ \frac{dg_Y}{dt} &= \frac{1}{16\pi^2} \left[\frac{41}{6} g_Y^3 \right],\end{aligned}\quad (49)$$

where $n_g = 3$ is the number of generations [100]. Finally, the running of f is driven by [101]

$$\frac{df}{dt} = \frac{f^3}{4\pi^2}. \quad (50)$$

V. VACUUM STABILITY CONSTRAINTS

We now proceed to study the vacuum stability of the model through numerical integration of Eqs. (47), (48), (49) and (50). To ensure perturbativity of f between the TeV scale and the Planck scale we find from (51),

$$f = \left(\frac{1}{f_0^2} - \frac{(t - t_0)}{2\pi^2} \right)^{-1/2}, \quad (51)$$

yielding $f_0 < 0.7$. For normalization, we set $t = \ln(Q/125 \text{ GeV})$ and $t_{\text{max}} = \ln(\Lambda/125 \text{ GeV})$. Now, using the SM relation $m_H^2 = -2\mu^2$, with $m_H \simeq 125 \text{ GeV}$, and setting $\langle \phi \rangle^2 = 246 \text{ GeV}$ at the same energy scale $Q = 125 \text{ GeV}$ we fix the initial conditions for the parameters μ and λ . Throughout we take the top Yukawa coupling renormalized at the top pole mass [102].

A. Light scalar singlet

We integrate the RG equations from $m_{h_2} = m_H$ and impose the initial conditions for $\lambda_{1,2,3}$ by putting the observed values into (16)

$$\langle \phi_{\text{SM}} \rangle^2 \Big|_{Q=m_{h_2}} = \langle \phi \rangle^2 \Big|_{Q=m_{h_2}}, \quad m_{h_2} = m_H. \quad (52)$$

The other quantities in (16) $m_{h_1} = m_h, \theta$ and $\langle r \rangle$ remain free parameters. It is easily seen through numerical integration of (47), (48), (49) and (50), that there are stable vacua up to the Planck scale. However, for those stable vacua, the required values of θ and m_h are excluded at 90% C.L.

As an illustration, we note that there is a stable solution for $\langle r \rangle = 2.8 \text{ GeV}$ and $m_h = 0.3 \text{ GeV}$, which corresponds $\theta = 0.01$. As can be seen in Fig. 2, this region of the parameter space is excluded at 90% C.L. Actually, for $m_h = 0.3 \text{ GeV}$, it can be shown that the mixing angle is bounded from below: $\theta > 0.004$. The argument is as follows. The Yukawa coupling f of the Majorana fermion does not suppress the growth of λ_2 , but does exactly the opposite. This is due to the smallness of f and therefore

$f^4 < 16\lambda_2^2 f^2$ in $d\lambda_2/dt$. As a result, we can simply set $f = 0$. The RG equation of λ_2 then implies a constraint on its boundary value: $\lambda_2|_{Q=m_H} < 0.2$ or it blows up before reaching the Planck scale. For $\lambda_2|_{Q=m_H} = 0.2$, we need $\lambda_3|_{Q=m_H} < -0.28$ to have λ_1 always positive. We note that a positive λ_3 only makes λ_1 grows slower and does not help the situation. A smaller $\lambda_2|_{Q=m_H}$ only slows down the growth of λ_3 and does not improve the stability. In other words, the maximum of $\lambda_3|_{Q=m_H}$ is -0.28 . Moreover, from (16) we see that the mixing angle decreases monotonically when either $\lambda_3|_{Q=m_H}$ (when it is negative) or $\lambda_2|_{Q=m_H}$ increases. So we reach a minimum angle when $\lambda_2|_{Q=m_H} = 0.2$ and $\lambda_3|_{Q=m_H} = -0.28$, which gives $\theta = 0.004$. Such a value is excluded at the 90% C.L.

Next, we show that for $m_h > 0.3 \text{ GeV}$, the required mixing angle for a stable vacuum up to the Planck scale is $\theta > 0.004$. To this end, we rewrite (16) as

$$\lambda_2 = \frac{m_H^2}{4y^2} 2x^2 + \frac{m_h^2}{4y^2} (2 - 2x^2), \quad (53)$$

$$\lambda_3 = 2x \frac{m_h^2 - m_H^2}{2\langle \phi \rangle y}, \quad (54)$$

where we have taken $x = \sin \theta$ and $y = \langle r \rangle$. Now, since $m_h < m_H$ by increasing m_h we decrease $|m_h^2 - m_H^2|$ and therefore from (54) we see that x/y increases. Consequently, the term

$$\frac{m_H^2}{4y^2} 2x^2 - \frac{m_h^2}{4y^2} 2x^2 \quad (55)$$

in (53) increases (because it is proportional to x^2/y^2) and therefore the other term $\propto 1/y^2$ decreases. In other words, we have both x/y and y rising and therefore $x(\theta)$ increases with increasing m_h .

It should be noted that a theoretical lower limit on the mass of the hidden scalar can be obtained by generalizing the Weinberg-Linde [103, 104] bound (see also [105]). Herein instead we have used experimental data to determine such a lower limit. For $m_h < 0.3 \text{ GeV}$, the previously derived lower bound on θ can be relaxed. However, for $m_h = 35 \text{ MeV}$, we cannot reduce the mixing angle to a level consistent with searches for the rare flavor-changing neutral-current decay $K^+ \rightarrow \pi^+ + \cancel{E}_T$ without sacrificing vacuum stability, *i.e.* $\lambda_3 \sim 1$ is required to obtain $\theta \lesssim 10^{-4}$. Moreover, the upper limit set by SN1987A observations excludes values of $m_h < 35 \text{ MeV}$, for $\lambda_2 \lesssim 0.2$. As an illustration, in Fig. 4 we show a comparison between the θ behavior imposed by vacuum stability and the upper limit on the mixing angle derived from (37), fixing the quartic coupling of the hidden scalar to the fiducial value that saturates the condition of vacuum stability, *i.e.* $\lambda_2 = 0.2$.

We conclude that, for $m_{h_2} = m_H$, there are no stable solutions up to the Planck scale in the allowed region of the parameter space.

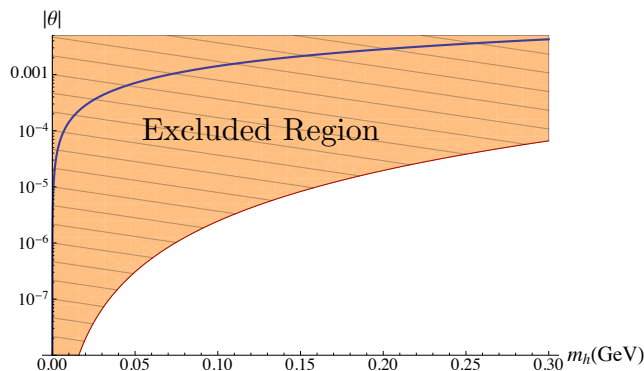


FIG. 4. Comparison of vacuum stability requirements in the (θ, m_h) plane (blue curve) with the upper limit set by SN1987A observations.

B. Heavy scalar singlet

For energies below the mass of the heavier Higgs h_2 , the effective theory is (of course) the SM. In the low energy regime the Higgs sector is given by

$$\mathcal{L}_{\text{SM}} \supset (\mathcal{D}_\mu \Phi)^\dagger (\mathcal{D}^\mu \Phi) - \mu^2 \Phi^\dagger \Phi - \lambda (\Phi^\dagger \Phi)^2, \quad (56)$$

and the RG equations are those of SM. To obtain the matching conditions connecting the two theories, following [26] we integrate out the field S to obtain a Lagrangian of the form (56). Identifying the quadratic and quartic terms in the potential yields

$$\mu^2 = \mu_1^2 - \mu_2^2 \frac{\lambda_3}{2\lambda_2} \quad (57)$$

and

$$\lambda = \lambda_1 \left(1 - \frac{\lambda_3^2}{4\lambda_1\lambda_2} \right), \quad (58)$$

respectively. This is consistent with the continuity of $\langle \phi_{\text{SM}} \rangle \Leftrightarrow \langle \phi \rangle$; namely

$$\langle \phi_{\text{SM}} \rangle^2 = - \frac{\mu^2}{\lambda} \Big|_{Q=m_{h_2}} = - \frac{\mu_1^2 - \frac{\mu_2^2 \lambda_3}{2\lambda_2}}{\lambda_1 \left(1 - \frac{\lambda_3^2}{4\lambda_1\lambda_2} \right)} \Big|_{Q=m_{h_2}},$$

or equivalently

$$\langle \phi_{\text{SM}} \rangle^2 \Big|_{Q=m_{h_2}} = \langle \phi \rangle^2 \Big|_{Q=m_{h_2}}, \quad (59)$$

with $\langle \phi \rangle$ given by (9). The quartic interaction between the heavy scalar singlet and the Higgs doublet provides an essential contribution for the stabilization the scalar field potential [26].

When we refer to the stability of (4) at some energy Q (with the use of the couplings at that scale), we are assuming that the field values are at the scale Q . Note that the field values are the only functional arguments when

talking about a potential like (4), and therefore the appropriate renormalization scale must also be at that scale. For $\lambda_3 > 0$, the third condition in (7) could potentially be violated only for field values $\langle \phi \rangle$ around m_{h_2} , regardless of the renormalization scale Q [26]. Consequently, the region of instability is found to be:

$$\begin{aligned} \langle r \rangle &< m_{h_2} / \sqrt{2\lambda_2}, \\ Q_- &< \langle \phi \rangle < Q_+, \\ Q_\pm^2 &= \frac{m_{h_2}^2 \lambda_3}{8\lambda_1 \lambda_2} \left(1 \pm \sqrt{1 - \frac{4\lambda_1 \lambda_2}{\lambda_3^2}} \right) \Big|_{Q_*}, \end{aligned} \quad (60)$$

where Q_* is some energy scale where the extra positivity condition is violated; see Appendix C.⁴ Therefore, $Q_\pm \sim m_{h_2}$ when the extra positivity condition is saturated, that is $\lambda_1 \lambda_2 = \lambda_3/4$. From (60) it follows that $Q_\pm \sim m_{h_2}$ when all the λ_i are roughly at the same scale. If one of the $\lambda_{1,2}$ is near zero, then Q_+ can be $\gg m_{h_2}$, but this region of the parameter space is constrained by the condition $\lambda_{1,2} > 0$. The stability for field values at scale m_{h_2} (instead of Q). Therefore, for $\lambda_3 > 0$, we impose the extra positivity condition in the vicinity of m_{h_2} . Even though the potential seems unstable at $Q \gg m_{h_2}$, it is actually stable when all the field values are at the scale Q . Note that the potential with $\lambda_i(Q)$ can only be used when the functional arguments (field values $\langle \phi \rangle, \langle r \rangle$) are at the scale Q . On the other hand, the instability region for $\lambda_3 < 0$ is given by

$$\begin{aligned} \langle r \rangle &> \frac{m_{h_2}}{\sqrt{2\lambda_2}}, \\ c_- &< \frac{\langle \phi \rangle}{\langle r \rangle} < c_+, \\ c_\pm^2 &= - \frac{\lambda_3}{2\lambda_1} \left(1 \pm \sqrt{1 - \frac{4\lambda_1 \lambda_2}{\lambda_3^2}} \right) \Big|_{Q_*}, \end{aligned} \quad (61)$$

and hence is given by the ratio of $\langle \phi \rangle$ and $\langle r \rangle$, which can be reached even with both $\langle \phi \rangle$ and $\langle r \rangle$ being $\gg m_{h_2}$; see Appendix C. Therefore, for $\lambda_3 < 0$, we impose the extra positivity condition at all energy scales. Note that the asymmetry in λ_3 will carry over into an asymmetry in θ .

To solve the system – (47), (48), (49) and (50) – we run the SM couplings from 125 GeV up to the mass scale m_{h_2} and use the matching conditions to determine $\langle \phi_{\text{SM}} \rangle$, which in turns allows one to solve algebraically for m_{h_1} . In Fig. 5 we compare the region of the parameter space which contains stable vacua up to the Planck scale

⁴ Note that (60) is where the potential can become negative. If the third condition in (7) is satisfied, Q_\pm will be imaginary, which implies that the potential is always positive. So we need to make sure the third condition is satisfied $Q_\pm \sim m_{h_2}$ so that the potential can never be negative. On the other hand, we only need to consider the third condition in this range as for other $\langle \phi \rangle$, the potential is positive regardless of the value of $\frac{1}{4}\lambda_3^2 - \lambda_1\lambda_2$.

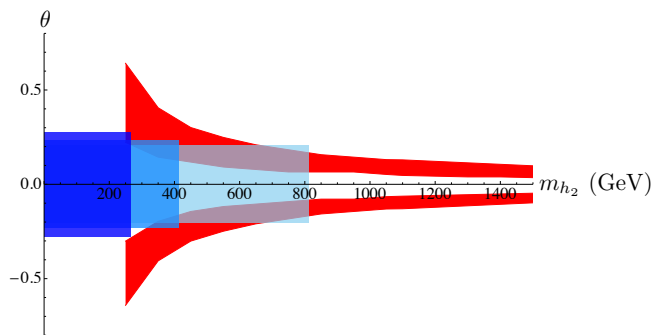


FIG. 5. The red area shows the allowed parameter space in the m_{h_2} vs. θ plane under the vacuum stability constraint of Eq. (7), with $\Lambda = 10^{19}$ GeV. The blue areas indicate the regions of the parameter space that are not excluded by direct DM searches for $f_0 = 0.4, 0.5, 0.7$, from light to dark shading. The perturbative upper bound is defined by $\lambda_i < 2\pi$.

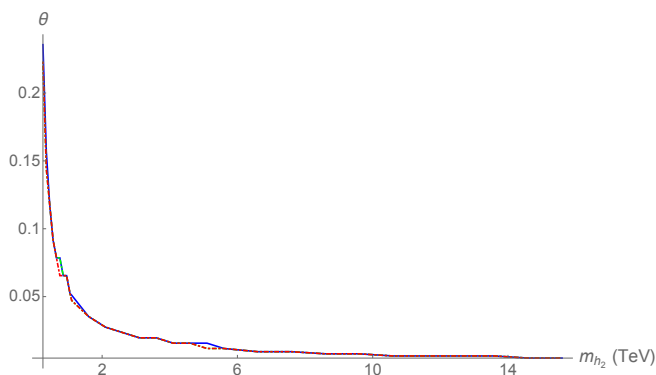


FIG. 6. Comparison of three solutions of stable vacua, with identical initial conditions except for $f_0 = 0.4$ (red dashed line), $f_0 = 0.5$ (green dot-dashed line), and $f_0 = 0.7$ (blue solid line).

(red area) with the allowed (blue) bands from direct DM searches. From (35) it is straightforward to see that the heaviest WIMP satisfying the relic density constraint, $m_w = 70$ TeV, is near the unitarity limit [56]. However, one can immediately recognize in Fig. 1 that such a WIMP mass exceeds the perturbativity limit, $f_0 \leq 0.7$. The maximum WIMP mass that simultaneously satisfies the relic density constraint in (35) and the f_0 perturbativity limit in (51) is $m_w = 1$ TeV. This maximum mass then determines the range of the darker blue band in the horizontal axis (m_{h_2}) of Fig. 5. The LUX upper bound on the WIMP-nucleon cross section for elastic scattering [58] via (38) sets an upper limit on the mixing angle. The allowed values of θ determine the range of the (blue) bands in the vertical axis of Fig. 5. The different blue bands correspond to three fiducial values of the Majorana coupling $f_0 = 0.4, 0.5, 0.7$. It is important to stress that the f_0 dependence of the RG running can be safely neglected; see Fig. 6. It is also important to stress that new physics thresholds, which may appear near the Planck mass, does not significantly mod-

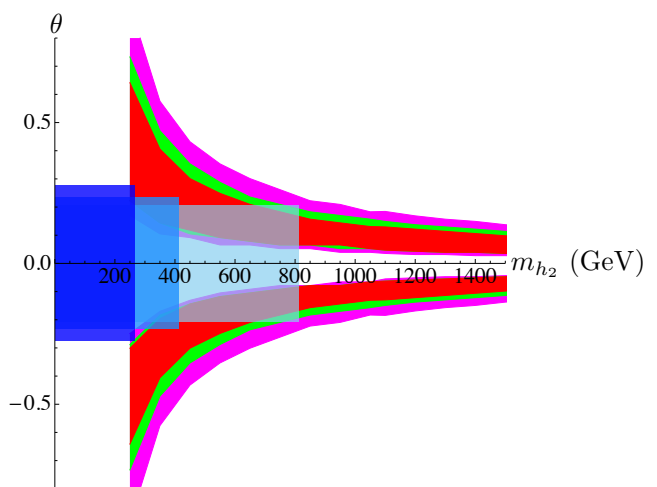


FIG. 7. The allowed parameter space in the m_{h_2} vs. θ plane under the vacuum stability constraint of Eq. (7), with $\Lambda = 10^{11}$ GeV (magenta), $\Lambda = 10^{15}$ GeV (green), and $\Lambda = 10^{19}$ GeV (red). The blue areas indicate the regions of the parameter space that are not excluded by direct DM searches for $f_0 = 0.4, 0.5, 0.7$, from light to dark shading. The perturbative upper bound is defined by $\lambda_i < 2\pi$.

ify the region of the parameter space with stable vacua, see Fig. 7. In summary, the superposition of the blue and red areas in Fig. 5 indicates the region of the parameter space which develops a stable vacuum, satisfies the relic density condition, and is in agreement with direct DM searches. The interesting region of the parameter space comprises WIMP masses $350 \text{ GeV} \lesssim m_w \lesssim 1 \text{ TeV}$.⁵ The region of interest is within reach of second generation DM direct detection experiments, such as DEAP3600, DarkSide G2, XENONnT, and DARWIN [108, 109].

VI. CONCLUSIONS

We have studied the vacuum stability of a minimal Higgs portal model in which the SM particle spectrum is extended to include one complex scalar field S and one Dirac fermion field ψ . These new fields are singlets under the SM gauge group and are charged under a global $U(1)$ symmetry: $U(1)_W(\psi) = 1$ and $U(1)_W(S) = 2$. The spontaneous breaking of this $U(1)$ symmetry results in a massless Goldstone boson, a massive CP -even scalar, and splits the Dirac fermion into two new mass-eigenstates ψ_{\pm} , corresponding to Majorana fermions. The symmetry breaking yields naturally a WIMP candidate. Fields with an even (odd) charge under the global $U(1)$ symmetry will acquire, after symmetry breaking, an even (odd)

⁵ Curiously, the ATLAS Collaboration has reported a 3σ excess of Higgs pair production $HH \rightarrow \gamma\gamma b\bar{b}$ for $m_{h_2} \sim 300$ GeV [106]. See also [107].

discrete charge under a Z_2 discrete symmetry. While the SM particles are all even under Z_2 , the Majorana fermions ψ_{\pm} are odd. In such a set up the lightest particle with odd charge, ψ_- , will be absolutely stable, and hence a plausible WIMP candidate.

We have shown that interactions between the extended Higgs sector and the lightest Majorana fermion which are strong enough to yield a thermal relic abundance consistent with observation can easily destabilize the electroweak vacuum or drive the theory into a non-perturbative regime at an energy scale well below the Planck mass. However, we have also unmasked a small region of the parameter space which develops a stable vacuum (up to the Planck scale), satisfies the relic abundance, and is in agreement with direct DM searches. This region comprises WIMP masses $350 \text{ GeV} \lesssim m_w \lesssim 1 \text{ TeV}$. The region of interest is within reach of second generation DM direct detection experiments.

Needless to say, here we have considered a minimal model to ensure that bounding the parameter space remains tractable. However, our extension of the dark sec-

tor enlarges the parameter space sufficiently to contain stable vacua up to the Planck scale.

ACKNOWLEDGMENTS

We thank Wai-Yee Keung and Neal Weiner for valuable discussions. LAA is supported by U.S. National Science Foundation (NSF) CAREER Award PHY1053663 and by the National Aeronautics and Space Administration (NASA) Grant No. NNX13AH52G; he thanks the Center for Cosmology and Particle Physics at New York University for its hospitality. VB is supported by the U. S. Department of Energy (DoE) Grant No. DE-FG-02-95ER40896. HG is supported by NSF Grant No. PHY-1314774. XH is supported by the MOST Grant 103-2811-M-003-024. DM is supported by DoE Grant No. de-sc0010504. TJW is supported by DoE Grant No. de-sc0011981 and the Simons Foundation Grant No. 306329.

Appendix A

To determine the value of G_q/m_q we look back at (24) along with the SM Yukawa interaction term, which involves the mixing of both scalar fields, h_1 and h_2 . For interactions of WIMPs with SM quarks, the relevant terms are

$$\mathcal{L} = \frac{m_q \cos \theta}{\langle \phi \rangle} h_{1,2} \bar{\psi}_q \psi_q - \frac{m_q \sin \theta}{\langle \phi \rangle} h_{2,1} \bar{\psi}_q \psi_q + \dots + \frac{f \sin \theta}{2} h_{1,2} \bar{\psi}_- \psi_- + \frac{f \cos \theta}{2} h_{2,1} \bar{\psi}_- \psi_-. \quad (\text{A1})$$

The scattering of a w particle off a quark then gives

$$\begin{aligned} \mathcal{M} &= i \frac{f m_q \sin \theta \cos \theta}{\langle \phi \rangle} \bar{u}_q(p') u_q(p) \left(\frac{1}{t - m_{h_{1,2}}^2} - \frac{1}{t - m_{h_{2,1}}^2} \right) \bar{u}(k') u(k) \\ &\approx i \frac{f m_q \lambda_3 \langle r \rangle}{m_{h_1}^2 m_{h_2}^2} \bar{u}_q(p') u_q(p) \bar{u}(k') u(k). \end{aligned} \quad (\text{A2})$$

This leads to the identification of the effective coupling

$$\frac{2G_q}{\sqrt{2}} = \frac{m_q f \lambda_3 \langle r \rangle}{m_{h_1}^2 m_{h_2}^2} \Rightarrow \frac{G_q}{m_q} = \frac{\sqrt{2} f \lambda_3 \langle r \rangle}{2 m_{h_1}^2 m_{h_2}^2}. \quad (\text{A3})$$

Appendix B

To establish the one-loop RG equations for the parameters of the scalar potential, we first compute the one-loop effective potential and then impose its independence from the renormalisation scale. To one-loop level, the scalar potential is given by $V = V^{(0)} + \Delta V^{(1)}$, where $V^{(0)}$ is the tree-level potential and $\Delta V^{(1)}$ indicates the one-loop correction to it. To compute the latter it is useful to re-write the tree-level potential (4) in terms of the real scalar fields:

$$\Phi = \frac{1}{\sqrt{2}} \begin{pmatrix} \varphi_1 + i\varphi_2 \\ \varphi_3 + i\varphi_4 \end{pmatrix} \quad \text{and} \quad S = \frac{1}{\sqrt{2}} (\varkappa_1 + i\varkappa_2). \quad (\text{B1})$$

The particular combination of fields relevant for the calculation are $\varphi^2 = \varphi_1^2 + \varphi_2^2 + \varphi_3^2 + \varphi_4^2$ and $\varkappa^2 = \varkappa_1^2 + \varkappa_2^2$; hence (4) can be rewritten as

$$V^{(0)}(\varphi, r) = \frac{1}{2} \mu_1^2 \varphi^2 + \frac{1}{2} \mu_2^2 \varkappa^2 + \frac{1}{4} \lambda_1 \varphi^4 + \frac{1}{4} \lambda_2 \varkappa^4 + \frac{1}{4} \lambda_3 \varphi^2 \varkappa^2. \quad (\text{B2})$$

In the Landau gauge the one-loop correction to the tree-level potential (B2) reads:

$$\Delta V^{(1)}(\varphi, \varkappa) = \frac{1}{64\pi^2} \sum_i (-1)^{2s_i} (2s_i + 1) M_i^4(\varphi^2, \varkappa^2) \left[\ln \frac{M_i^2(\varphi^2, \varkappa^2)}{Q^2} - c_i \right], \quad (\text{B3})$$

where c_i are constants that depend on the renormalisation scheme. For the $\overline{\text{MS}}$ scheme, we have $c_i = 5/6$ for vectors, and $c_i = 3/2$ for scalars and fermions. Next, we expand (B3) and we just keep the contributions from the scalar fields, the top-quark, the gauge bosons, and the Majorana fermions,

$$\begin{aligned} \Delta V^{(1)} = & \frac{1}{64\pi^2} \left\{ 3\mathcal{G}_1^2 \left[\ln \frac{\mathcal{G}_1}{Q^2} - \frac{3}{2} \right] + \mathcal{G}_2^2 \left[\ln \frac{\mathcal{G}_2}{Q^2} - \frac{3}{2} \right] + \text{Tr} \left(\mathcal{H}^2 \left[\ln \frac{\mathcal{H}}{Q^2} - \frac{3}{2} \right] \right) - 12 T_\varphi^2 \left[\ln \frac{T_\varphi}{Q^2} - \frac{3}{2} \right] \right. \\ & \left. + 3\text{Tr} \left(M_\varphi^2 \left[\ln \frac{M_\varphi}{Q^2} - \frac{5}{6} \right] \right) - 4W_\varkappa^2 \left[\ln \frac{W_\varkappa}{Q^2} - \frac{3}{2} \right] \right\}, \end{aligned} \quad (\text{B4})$$

where (in a self-explanatory notation) the field-dependent squared masses are,

$$\mathcal{G}_1(\varphi, \varkappa) = \mu_1^2 + \lambda_1 \varphi^2 + \frac{\lambda_3}{2} \varkappa^2, \quad (\text{B5})$$

$$\mathcal{G}_2(\varphi, \varkappa) = \mu_2^2 + \lambda_2 \varkappa^2 + \frac{\lambda_3}{2} \varphi^2, \quad (\text{B6})$$

$$\mathcal{H}(\varphi, \varkappa) = \begin{pmatrix} \mu_1^2 + 3\lambda_1 \varphi^2 + \frac{\lambda_3}{2} \varkappa^2 & \lambda_3 \varphi \varkappa \\ \lambda_3 \varphi \varkappa & \mu_2^2 + 3\lambda_2 \varkappa^2 + \frac{\lambda_3}{2} \varphi^2 \end{pmatrix}, \quad (\text{B7})$$

$$T_\varphi(\varphi) = \frac{1}{2} (Y_t \varphi)^2, \quad (\text{B8})$$

$$M_\varphi(\varphi) = \frac{1}{4} \begin{pmatrix} g_Y^2 \varphi^2 & -g_2 g_Y \varphi^2 \\ -g_2 g_Y \varphi^2 & g_2^2 \varphi^2 \end{pmatrix}, \quad (\text{B9})$$

$$W_\varkappa(\varkappa) = \frac{1}{4} (f \varkappa)^2. \quad (\text{B10})$$

We define the beta functions β_i ($i = 1 \dots 3$) for the quartic couplings, the gamma functions γ_{μ_1, μ_2} for the scalar masses, and the scalar anomalous dimensions $\gamma_{\varphi, \varkappa}$ according to: $d\lambda_i/dt = \beta_i$, $d\mu_1^2/dt = \gamma_{\mu_1} \mu_1^2$, $d\mu_2^2/dt = \gamma_{\mu_2} \mu_2^2$, $d\varphi^2/dt = 2\gamma_\varphi \varphi^2$, and $d\varkappa^2/dt = 2\gamma_\varkappa \varkappa^2$. We then extract the RG equations for the parameters of the scalar potential by forcing the first derivative of the effective potential with respect to the scale t to vanish

$$\frac{d}{dt} V^{(1)} \equiv \frac{d}{dt} (V^{(0)} + \Delta V^{(1)}) \equiv 0, \quad (\text{B11})$$

keeping only the one-loop terms. After a bit of algebra (B11) leads to the following equations:

$$\begin{aligned} \frac{\mu_1^2 \varphi^2}{2} \left[\gamma_{\mu_1} + 2\gamma_\varphi - \frac{1}{16\pi^2} \left(12\lambda_1 + 2\frac{\mu_2^2}{\mu_1^2} \lambda_3 \right) \right] &= 0, \\ \frac{\mu_2^2 \varkappa^2}{2} \left[\gamma_{\mu_2} + 2\gamma_\varkappa - \frac{1}{16\pi^2} \left(8\lambda_2 + 4\frac{\mu_1^2}{\mu_2^2} \lambda_3 \right) \right] &= 0, \\ \frac{\varphi^4}{4} \left[\beta_1 + 4\lambda_1 \gamma_\varphi - \frac{1}{16\pi^2} \left(24\lambda_1^2 + \lambda_3^2 - 6Y_t^4 + \frac{9}{8}g_2^4 + \frac{3}{8}g_Y^4 + \frac{3}{4}g_2^2 g_Y^2 \right) \right] &= 0, \\ \frac{\varkappa^4}{4} \left[\beta_2 + 4\lambda_2 \gamma_\varkappa - \frac{1}{8\pi^2} \left(10\lambda_2^2 + \lambda_3^2 - \frac{1}{4}f^4 \right) \right] &= 0, \\ \frac{\varphi^2 \varkappa^2}{4} \left[\beta_3 + 2\lambda_3 (\gamma_\varphi + \gamma_\varkappa) - \frac{1}{8\pi^2} (6\lambda_1 \lambda_3 + 4\lambda_2 \lambda_3 + 2\lambda_3^2) \right] &= 0. \end{aligned} \quad (\text{B12})$$

Requiring that each term between squared brackets vanishes, we arrive at the RG equations for the parameters of the scalar potential. Namely, substituting the explicit expression of the scalar anomalous dimensions [8]

$$\gamma_\varphi = -\frac{1}{16\pi^2} \left(3Y_t^2 - \frac{9}{4}g_2^2 - \frac{3}{4}g_Y^2 \right) \quad \text{and} \quad \gamma_\varkappa = -\frac{1}{8\pi^2} f^2, \quad (\text{B13})$$

into (B12) we obtain (47).

Appendix C

To explore the impact of the complex singlet scalar on the stability of the Higgs sector we follow [26] and consider a tree level scalar potential of the form

$$V(\Phi, S) = \lambda_1 \left(\Phi^\dagger \Phi - \frac{\langle \phi \rangle^2}{2} \right)^2 + \lambda_2 \left(S^\dagger S - \frac{\langle r \rangle^2}{2} \right)^2 + \lambda_3 \left(\Phi^\dagger \Phi - \frac{\langle \phi \rangle^2}{2} \right) \left(S^\dagger S - \frac{\langle r \rangle^2}{2} \right). \quad (\text{C1})$$

For $\lambda_3 > 0$, the third term can only be negative when either one of the factors is negative. The parameter space for $\Phi^\dagger \Phi < \langle \phi \rangle^2/2$ is, in principle, described by the effective potential of the SM (with one Higgs). So herein we only consider $S^\dagger S < \langle r \rangle^2/2$. As argued in [26], the most dangerous region of the field configuration is given by $S = 0$.⁶ In this region, we have

$$V(\Phi, 0) = \lambda_1(Q) \left(|\Phi|^2 - \frac{\langle \phi \rangle^2}{2} \right)^2 + \lambda_2(Q) \left(\frac{\langle r \rangle^2}{2} \right)^2 - \frac{\langle r \rangle^2}{2} \lambda_3(Q) \left(|\Phi|^2 - \frac{\langle \phi \rangle^2}{2} \right). \quad (\text{C2})$$

The couplings are now replaced by their values at some scale Q . We take $\langle \phi \rangle$ and $\langle r \rangle$ to be the physical VEV and only the couplings λ_i run. This is possible in some renormalization scheme (like taking vacuum expectation $|\Phi| = \langle \phi \rangle, |S| = \langle r \rangle$ as one of the renormalization conditions, which is satisfied trivially for this particular form of potential). Keeping only terms with $\langle r \rangle$ (since $\langle r \rangle \gg \langle \phi \rangle$), the condition $V = 0$ can be rewritten as,

$$\lambda_1(Q) |\Phi|^4 + \frac{\lambda_2(Q) \langle r \rangle^4}{4} - \frac{\lambda_3(Q) \langle r \rangle^2}{2} |\Phi|^2 = 0. \quad (\text{C3})$$

Next, we assume that $\lambda_2(Q) \langle r \rangle^2 \sim -\mu_2(Q)^2$ is almost unchanged under the RG flow and remains $\frac{1}{2} m_{h_2}^2$ (*i.e.* we assume that λ_i does not run by much). Under this assumption (C3) becomes

$$\lambda_1(Q) |\Phi|^4 - \frac{\lambda_3(Q) m_{h_2}^2}{4 \lambda_2(Q)} |\Phi|^2 + \frac{m_{h_2}^4}{16 \lambda_2(Q)} = 0. \quad (\text{C4})$$

The solution to this equation gives Eq. (60); the first condition comes from $|S|^2 < \langle r \rangle^2/2 \sim \frac{1}{2} m_{h_2}^2$, with $\langle \phi \rangle = \sqrt{2} |\Phi|$ [26].

For $\lambda_3 < 0$, we can consider a field configuration with both $|\Phi| \sim Q, |S| \sim Q$ much larger than $\langle r \rangle$. The point is that we only need to find a configuration in which the stability is violated. In this case, we must keep only the quartic term and the potential becomes

$$V(\Phi, S) = \lambda_1 |\Phi|^4 + \lambda_2 |S|^4 + \lambda_3 |\Phi|^2 |S|^2. \quad (\text{C5})$$

On the one hand, following [26] we can duplicate the procedure to obtain (62). These conditions can be satisfied and therefore the vacuum becomes unstable. On the other hand, we can just consider the eigenvalues of the matrix

$$\begin{pmatrix} \lambda_1 & \frac{1}{2} \lambda_3 \\ \frac{1}{2} \lambda_3 & \lambda_2 \end{pmatrix}. \quad (\text{C6})$$

In fact, the second approach also tells us why in the case of $\lambda_3 > 0$, a potential with the form of (C5) is in fact stable. The eigenvector with the negative eigenvalue is given by

$$\left(-\frac{-\lambda_1 + \lambda_2 + \sqrt{\lambda_1^2 - 2\lambda_1\lambda_2 + \lambda_2^2 + \lambda_3^2}}{\lambda_3}, 1 \right)$$

When $\lambda_3^2 \geq 4\lambda_1\lambda_2$, the first component is negative. So it requires either $|\Phi|^2$ or $|S|^2$ to be negative, which is impossible. As a result, for $\lambda_3 > 0$ we need to consider a particular field configuration to study the instability.

⁶ The instability region is defined by both relations $Q_- < \Phi < Q_+$ and $\lambda_1\lambda_2 < (2\lambda_3)^{-2}$, with the couplings evaluated at the scale Φ . The second relation is more likely to be satisfied at a high

energy scale, and therefore $|\Phi| = Q_+$ is the most dangerous region of the field configuration to reach the instability region, *i.e.* $V(\Phi, S) = 0$.

We now relate the two functional forms of the Higgs potential. At the classical level (4) differs from (C1) by a constant; that is the vacuum energy is shifted. In fact (4) has a negative vacuum energy $\sim -\frac{1}{4}\lambda_2(\langle r \rangle)\langle r \rangle^4$ (again neglecting all $\langle \phi \rangle$ corrections) and the instability requires the potential to be smaller than this negative vacuum energy.

At a particular scale Q , all the couplings λ_i in (4) can be replaced by $\lambda_i(Q)$ and $\mu_{1,2}(Q)$, so that (4) can be rewritten in the form of (C1) with some $\langle \phi(Q) \rangle, \langle r(Q) \rangle$ as a combination of $\lambda_i(Q)$ and $\mu_i(Q)$. Note that we can still adopt our previous arguments to consider only the configuration $|S| = 0$. In this case,

$$V(\Phi, 0) = \mu_1^2(Q) |\Phi|^2 + \lambda_1(Q) |\Phi|^4 \quad (\text{C7})$$

The condition for stability is saturated when

$$\mu_1^2(Q) |\Phi|^2 + \lambda_1(Q) |\Phi|^4 + \frac{1}{4}\lambda_2(\langle r \rangle) \langle r \rangle^4 = 0. \quad (\text{C8})$$

Solving (10) we have $-\mu_1^2(\langle r \rangle) = \frac{1}{2}\lambda_3(\langle r \rangle) \langle r \rangle^2$. Now, assuming that all the λ_i do not run too much along the RG flow we obtain (C4).

When $\lambda_{1,2}$ remains relative away from zero, (60) remains a reasonable approximation for the scale Q_{\pm} between which (*i.e.*, $Q_- < \sqrt{2}|\Phi| < Q_+$) the potential can become negative. Note that a naïve argument for instability using only the quartic potential (which is usually how we get to $\lambda_3^2 \geq 4\lambda_1\lambda_2$) is only valid for $\lambda_3 < 0$. As a result, the potential can only become unstable in a some very particular field configuration. In this region, however, the effective potential is not valid since the field values are far away from the scale Q .

-
- [1] G. Aad *et al.* [ATLAS Collaboration], Phys. Lett. B **710**, 49 (2012) [arXiv:1202.1408 [hep-ex]].
- [2] S. Chatrchyan *et al.* [CMS Collaboration], Phys. Lett. B **710**, 26 (2012) [arXiv:1202.1488 [hep-ex]].
- [3] G. Aad *et al.* [ATLAS Collaboration], Phys. Lett. B **726**, 88 (2013) [Phys. Lett. B **734**, 406 (2014)] [arXiv:1307.1427 [hep-ex]].
- [4] S. Chatrchyan *et al.* [CMS Collaboration], Phys. Rev. D **89**, 092007 (2014) [arXiv:1312.5353 [hep-ex]].
- [5] G. Aad *et al.* [ATLAS Collaboration], Phys. Rev. D **90**, 052004 (2014) [arXiv:1406.3827 [hep-ex]].
- [6] V. Khachatryan *et al.* [CMS Collaboration], Eur. Phys. J. C **74**, 3076 (2014) [arXiv:1407.0558 [hep-ex]].
- [7] M. Lindner, M. Sher and H. W. Zaglauer, Phys. Lett. B **228**, 139 (1989).
- [8] M. Sher, Phys. Rept. **179**, 273 (1989).
- [9] M. A. Diaz, T. A. ter Veldhuis and T. J. Weiler, Phys. Rev. Lett. **74**, 2876 (1995) [hep-ph/9408319].
- [10] J. A. Casas, J. R. Espinosa and M. Quiros, Phys. Lett. B **342**, 171 (1995) [hep-ph/9409458].
- [11] M. A. Diaz, T. A. ter Veldhuis and T. J. Weiler, Phys. Rev. D **54**, 5855 (1996) [hep-ph/9512229].
- [12] J. A. Casas, J. R. Espinosa and M. Quiros, Phys. Lett. B **382**, 374 (1996) [hep-ph/9603227].
- [13] G. Isidori, G. Ridolfi and A. Strumia, Nucl. Phys. B **609**, 387 (2001) [hep-ph/0104016].
- [14] G. Isidori, V. S. Rychkov, A. Strumia and N. Tetradis, Phys. Rev. D **77**, 025034 (2008) [arXiv:0712.0242 [hep-ph]].
- [15] L. J. Hall and Y. Nomura, JHEP **1003**, 076 (2010) [arXiv:0910.2235 [hep-ph]].
- [16] J. Ellis, J. R. Espinosa, G. F. Giudice, A. Hoecker and A. Riotto, Phys. Lett. B **679**, 369 (2009) [arXiv:0906.0954 [hep-ph]].
- [17] J. Elias-Miro, J. R. Espinosa, G. F. Giudice, G. Isidori, A. Riotto and A. Strumia, Phys. Lett. B **709**, 222 (2012) [arXiv:1112.3022 [hep-ph]].
- [18] F. Bezrukov, M. Y. Kalmykov, B. A. Kniehl and M. Shaposhnikov, JHEP **1210**, 140 (2012) [arXiv:1205.2893 [hep-ph]].
- [19] G. Degrassi, S. Di Vita, J. Elias-Miro, J. R. Espinosa, G. F. Giudice, G. Isidori and A. Strumia, JHEP **1208**, 098 (2012) [arXiv:1205.6497 [hep-ph]].
- [20] D. Buttazzo, G. Degrassi, P. P. Giardino, G. F. Giudice, F. Sala, A. Salvio and A. Strumia, JHEP **1312**, 089 (2013) [arXiv:1307.3536 [hep-ph]].
- [21] V. Branchina and E. Messina, Phys. Rev. Lett. **111**, 241801 (2013) [arXiv:1307.5193 [hep-ph]].
- [22] V. Branchina, E. Messina and M. Sher, Phys. Rev. D **91**, 013003 (2015) [arXiv:1408.5302 [hep-ph]].
- [23] Z. Lalak, M. Lewicki and P. Olszewski, JHEP **1405**, 119 (2014) [arXiv:1402.3826 [hep-ph]].
- [24] L. Basso, S. Moretti and G. M. Pruna, Phys. Rev. D **82**, 055018 (2010) [arXiv:1004.3039 [hep-ph]].
- [25] M. Kadastik, K. Kannike, A. Racioppi and M. Raidal, JHEP **1205**, 061 (2012) [arXiv:1112.3647 [hep-ph]].
- [26] J. Elias-Miro, J. R. Espinosa, G. F. Giudice, H. M. Lee and A. Strumia, JHEP **1206**, 031 (2012) [arXiv:1203.0237 [hep-ph]].
- [27] C. Cheung, M. Papucci and K. M. Zurek, JHEP **1207**, 105 (2012) [arXiv:1203.5106 [hep-ph]].
- [28] L. A. Anchordoqui, I. Antoniadis, H. Goldberg, X. Huang, D. Lust, T. R. Taylor and B. Vlcek, JHEP **1302**, 074 (2013) [arXiv:1208.2821 [hep-ph]].
- [29] S. Baek, P. Ko, W. I. Park and E. Senaha, JHEP **1211**, 116 (2012) [arXiv:1209.4163 [hep-ph]].
- [30] W. Chao, M. Gonderinger and M. J. Ramsey-Musolf, Phys. Rev. D **86**, 113017 (2012) [arXiv:1210.0491 [hep-ph]].
- [31] C. Coriano, L. Delle Rose and C. Marzo, Phys. Lett. B **738**, 13 (2014) [arXiv:1407.8539 [hep-ph]].
- [32] W. Altmannshofer, W. A. Bardeen, M. Bauer, M. Carena and J. D. Lykken, JHEP **1501**, 032 (2015) [arXiv:1408.3429 [hep-ph]].

- [33] A. Falkowski, C. Gross and O. Lebedev, JHEP **1505**, 057 (2015) [arXiv:1502.01361 [hep-ph]].
- [34] J. Krog and C. T. Hill, arXiv:1506.02843 [hep-ph].
- [35] L. D. Rose, C. Marzo and A. Urbano, arXiv:1506.03360 [hep-ph].
- [36] J. L. Feng, Ann. Rev. Astron. Astrophys. **48**, 495 (2010) [arXiv:1003.0904 [astro-ph.CO]].
- [37] R. Schabinger and J. D. Wells, Phys. Rev. D **72**, 093007 (2005) [hep-ph/0509209].
- [38] B. Patt and F. Wilczek, hep-ph/0605188.
- [39] V. Barger, P. Langacker, M. McCaskey, M. J. Ramsey-Musolf and G. Shaughnessy, Phys. Rev. D **77**, 035005 (2008) [arXiv:0706.4311 [hep-ph]].
- [40] V. Barger, P. Langacker, M. McCaskey, M. Ramsey-Musolf and G. Shaughnessy, Phys. Rev. D **79**, 015018 (2009) [arXiv:0811.0393 [hep-ph]].
- [41] L. M. Krauss and F. Wilczek, Phys. Rev. Lett. **62**, 1221 (1989).
- [42] S. Weinberg, Phys. Rev. Lett. **110**, 241301 (2013) [arXiv:1305.1971 [astro-ph.CO]].
- [43] P. Sikivie, Phys. Rev. Lett. **48**, 1156 (1982).
- [44] A. Vilenkin and A. E. Everett, Phys. Rev. Lett. **48**, 1867 (1982).
- [45] M. S. Turner and F. Wilczek, Phys. Rev. Lett. **66**, 5 (1991).
- [46] G. R. Dvali, Phys. Lett. B **265**, 64 (1991).
- [47] T. Hiramatsu, M. Kawasaki, K. i. Saikawa and T. Sekiguchi, JCAP **1301**, 001 (2013) [arXiv:1207.3166 [hep-ph]].
- [48] J. R. Ellis, A. Ferstl and K. A. Olive, Phys. Lett. B **481**, 304 (2000) [hep-ph/0001005].
- [49] M. Beltran, D. Hooper, E. W. Kolb and Z. C. Krusberg, Phys. Rev. D **80**, 043509 (2009) [arXiv:0808.3384 [hep-ph]].
- [50] R. J. Hill and M. P. Solon, Phys. Rev. D **91**, 043505 (2015) [arXiv:1409.8290 [hep-ph]]. See, in particular, Table 10.
- [51] P. Junnarkar and A. Walker-Loud, Phys. Rev. D **87**, 114510 (2013) [arXiv:1301.1114 [hep-lat]].
- [52] L. A. Anchordoqui and B. J. Vlcek, Phys. Rev. D **88**, 043513 (2013) [arXiv:1305.4625 [hep-ph]].
- [53] K. A. Olive *et al.* [Particle Data Group Collaboration], Chin. Phys. C **38**, 090001 (2014).
- [54] C. Garcia-Cely, A. Ibarra and E. Molinaro, JCAP **1311**, 061 (2013) [arXiv:1310.6256 [hep-ph]].
- [55] P. Gondolo and G. Gelmini, Nucl. Phys. B **360**, 145 (1991).
- [56] K. Griest and M. Kamionkowski, Phys. Rev. Lett. **64**, 615 (1990).
- [57] K. Blum, Y. Cui and M. Kamionkowski, arXiv:1412.3463 [hep-ph].
- [58] D. S. Akerib *et al.* [LUX Collaboration], Phys. Rev. Lett. **112**, 091303 (2014) [arXiv:1310.8214 [astro-ph.CO]].
- [59] R. Agnese *et al.* [SuperCDMS Collaboration], Phys. Rev. Lett. **112**, 241302 (2014) [arXiv:1402.7137 [hep-ex]].
- [60] K. Choi *et al.* [Super-Kamiokande Collaboration], Phys. Rev. Lett. **114**, 141301 (2015) [arXiv:1503.04858 [hep-ex]].
- [61] K. Schmidt-Hoberg, F. Staub and M. W. Winkler, Phys. Lett. B **727**, 506 (2013) [arXiv:1310.6752 [hep-ph]].
- [62] J. D. Clarke, R. Foot and R. R. Volkas, JHEP **1402**, 123 (2014) [arXiv:1310.8042 [hep-ph]].
- [63] L. A. Anchordoqui, P. B. Denton, H. Goldberg, T. C. Paul, L. H. M. Da Silva, B. J. Vlcek and T. J. Weiler, Phys. Rev. D **89**, 083513 (2014) [arXiv:1312.2547 [hep-ph]].
- [64] P. del Amo Sanchez *et al.* [BaBar Collaboration], Phys. Rev. Lett. **107**, 021804 (2011) [arXiv:1007.4646 [hep-ex]].
- [65] F. P. Huang, C. S. Li, D. Y. Shao and J. Wang, arXiv:1307.7458 [hep-ph].
- [66] B. Aubert *et al.* [BaBar Collaboration], arXiv:0808.0017 [hep-ex].
- [67] J. Insler *et al.* [CLEO Collaboration], Phys. Rev. D **81**, 091101 (2010) [arXiv:1003.0417 [hep-ex]].
- [68] D. Buskulic *et al.* [ALEPH Collaboration], Phys. Lett. B **313**, 312 (1993).
- [69] M. Acciarri *et al.* [L3 Collaboration], Phys. Lett. B **385**, 454 (1996).
- [70] G. Alexander *et al.* [OPAL Collaboration], Phys. Lett. B **377**, 273 (1996).
- [71] G. Abbiendi *et al.* [OPAL Collaboration], Eur. Phys. J. C **27**, 311 (2003) [hep-ex/0206022].
- [72] G. Abbiendi *et al.* [OPAL Collaboration], Phys. Lett. B **682**, 381 (2010) [arXiv:0707.0373 [hep-ex]].
- [73] K. Cheung, W. Y. Keung and T. C. Yuan, Phys. Rev. D **89**, 015007 (2014) [arXiv:1308.4235 [hep-ph]].
- [74] B. Aubert *et al.* [BaBar Collaboration], Phys. Rev. Lett. **94**, 101801 (2005) [hep-ex/0411061].
- [75] P. del Amo Sanchez *et al.* [BaBar Collaboration], Phys. Rev. D **82**, 112002 (2010) [arXiv:1009.1529 [hep-ex]].
- [76] J. P. Lees *et al.* [BaBar Collaboration], Phys. Rev. D **87**, 112005 (2013) [arXiv:1303.7465 [hep-ex]].
- [77] T. E. Browder *et al.* [CLEO Collaboration], Phys. Rev. Lett. **86**, 2950 (2001) [hep-ex/0007057].
- [78] O. Lutz *et al.* [Belle Collaboration], Phys. Rev. D **87**, 111103 (2013) [arXiv:1303.3719 [hep-ex]].
- [79] S. Adler *et al.* [E787 Collaboration], Phys. Rev. Lett. **88**, 041803 (2002) [hep-ex/0111091].
- [80] V. V. Anisimovsky *et al.* [E949 Collaboration], Phys. Rev. Lett. **93**, 031801 (2004) [hep-ex/0403036].
- [81] S. Adler *et al.* [E949 and E787 Collaborations], Phys. Rev. D **77**, 052003 (2008) [arXiv:0709.1000 [hep-ex]].
- [82] A. V. Artamonov *et al.* [BNL-E949 Collaboration], Phys. Rev. D **79**, 092004 (2009) [arXiv:0903.0030 [hep-ex]].
- [83] V. Barger, M. Ishida and W. Y. Keung, Phys. Rev. Lett. **108**, 261801 (2012) [arXiv:1203.3456 [hep-ph]].
- [84] J. R. Espinosa, M. Muhlleitner, C. Grojean and M. Trott, JHEP **1209**, 126 (2012) [arXiv:1205.6790 [hep-ph]].
- [85] K. Cheung, J. S. Lee and P. -Y. Tseng, JHEP **1305**, 134 (2013) [arXiv:1302.3794 [hep-ph]].
- [86] P. P. Giardino, K. Kannike, I. Masina, M. Raidal and A. Strumia, JHEP **1405**, 046 (2014) [arXiv:1303.3570 [hep-ph]].
- [87] J. Ellis and T. You, JHEP **1306**, 103 (2013) [arXiv:1303.3879 [hep-ph]].
- [88] G. G. Raffelt, Phys. Rept. **198**, 1 (1990).
- [89] W. Y. Keung, K. W. Ng, H. Tu and T. C. Yuan, Phys. Rev. D **90**, 075014 (2014) [arXiv:1312.3488 [hep-ph]].
- [90] V. Khachatryan *et al.* [CMS Collaboration], Eur. Phys. J. C **75**, no. 5, 235 (2015) [arXiv:1408.3583 [hep-ex]].
- [91] L. Lopez-Honorez, T. Schwetz and J. Zupan, Phys. Lett. B **716**, 179 (2012) [arXiv:1203.2064 [hep-ph]].
- [92] L. Carpenter, A. DiFranzo, M. Mulhearn, C. Shimmin,

- S. Tulin and D. Whiteson, Phys. Rev. D **89**, 075017 (2014) [arXiv:1312.2592 [hep-ph]].
- [93] J. Abdallah *et al.*, arXiv:1506.03116 [hep-ph].
- [94] G. Steigman, D.N. Schramm and J.E. Gunn, Phys. Lett. B **66**, 202 (1977).
- [95] P. A. R. Ade *et al.* [Planck Collaboration], arXiv:1502.01589 [astro-ph.CO].
- [96] G. Mangano, G. Miele, S. Pastor, T. Pinto, O. Pisanti and P. D. Serpico, Nucl. Phys. B **729**, 221 (2005) [hep-ph/0506164].
- [97] E. Aver, K. A. Olive, R. L. Porter and E. D. Skillman, JCAP **1311**, 017 (2013) [arXiv:1309.0047 [astro-ph.CO]].
- [98] R. Cooke, M. Pettini, R. A. Jorgenson, M. T. Murphy and C. C. Steidel, arXiv:1308.3240 [astro-ph.CO].
- [99] K. M. Nollett and G. Steigman, Phys. Rev. D **91**, 083505 (2015) [arXiv:1411.6005 [astro-ph.CO]].
- [100] H. Arason, D. J. Castano, B. Keszthelyi, S. Mikaelian, E. J. Piard, P. Ramond and B. D. Wright, Phys. Rev. D **46**, 3945 (1992).
- [101] S. Iso, N. Okada and Y. Orikasa, Phys. Lett. B **676**, 81 (2009) [arXiv:0902.4050 [hep-ph]].
- [102] J. A. Casas, J. R. Espinosa, M. Quiros and A. Riotto, Nucl. Phys. B **436**, 3 (1995) [Erratum-ibid. B **439**, 466 (1995)] [hep-ph/9407389].
- [103] S. Weinberg, Phys. Rev. Lett. **36**, 294 (1976).
- [104] A. D. Linde, Phys. Lett. B **62**, 435 (1976).
- [105] M. Sher, Phys. Lett. B **317**, 159 (1993) [Phys. Lett. B **331**, 448 (1994)] [hep-ph/9307342].
- [106] G. Aad *et al.* [ATLAS Collaboration], Phys. Rev. Lett. **114**, 081802 (2015) [arXiv:1406.5053 [hep-ex]].
- [107] V. Khachatryan *et al.* [CMS Collaboration], arXiv:1503.04114 [hep-ex].
- [108] J. L. Feng *et al.*, arXiv:1401.6085 [hep-ex].
- [109] L. Baudis, Phys. Dark Univ. **4**, 50 (2014) [arXiv:1408.4371 [astro-ph.IM]].